



HAL
open science

Parameter identification for the shallow water equations using modal decomposition

Q. Wu, S. Amin, Simon Munier, Aurélie Bayen-Poisson, X. Litrico, Gilles
Belaud

► **To cite this version:**

Q. Wu, S. Amin, Simon Munier, Aurélie Bayen-Poisson, X. Litrico, et al.. Parameter identification for the shallow water equations using modal decomposition. 46th IEEE Conference on Decision and Control, Dec 2007, New Orléans, Louisiana, United States. 7 p. hal-00468546

HAL Id: hal-00468546

<https://hal.science/hal-00468546>

Submitted on 31 Mar 2010

HAL is a multi-disciplinary open access archive for the deposit and dissemination of scientific research documents, whether they are published or not. The documents may come from teaching and research institutions in France or abroad, or from public or private research centers.

L'archive ouverte pluridisciplinaire **HAL**, est destinée au dépôt et à la diffusion de documents scientifiques de niveau recherche, publiés ou non, émanant des établissements d'enseignement et de recherche français ou étrangers, des laboratoires publics ou privés.

Parameter identification for the shallow water equations using modal decomposition

Qingfang Wu[‡], Saurabh Amin[‡], Simon Munier[†], Alexandre M. Bayen[‡], Xavier Litrico[†] and Gilles Belaud^{*}

Abstract—A parameter identification problem for systems governed by first-order, linear hyperbolic partial differential equations subjected to periodic forcing is investigated. The problem is posed as a PDE constrained optimization problem with data of the problem given by the measured input and output variables at the boundary of the domain. By using the governing equations in the frequency domain, a spatially dependent transfer matrix relating the input variables to the output variables is obtained. It is shown that by considering a finite number of dominant oscillatory modes of the input, an accurate representation of the output can be obtained. This converts the original PDE constrained optimization problem to one without any constraints. The optimal parameters can be identified using standard nonlinear programming. The utility of the proposed approach is illustrated by considering a river reach in the Sacramento–San-Joaquin Delta, California, that is subjected to tidal forcing. The dynamics of the reach are modeled by linearized Saint-Venant equations. The available data is the flow variables measured upstream and downstream of the reach. The parameter identification problem is to estimate the average free-surface width, the bed slope, the friction coefficient and the steady-state boundary conditions. It is shown that the estimated model gives an accurate prediction of the flow variables at an intermediate location within the reach.

I. INTRODUCTION

Inverse problems arise frequently in the experimental study of a large-scale physical systems [1]. These problems aim at discerning the dynamics that govern the system based on the available data collected by monitoring devices. One of the most well-studied inverse problem is the *parameter identification* problem for finite-dimensional systems in which the task is to estimate the unknown parameters of an *ordinary differential equation* (ODE) [2]. Parameter identification for systems modeled by *partial differential equations* (PDEs) is fundamentally different than the case of ODEs because of the presence of spatial derivatives in the system model and the dependence of coefficients on the space variable.

An example that motivates the study of parameter identification for PDEs arises in open-channel hydraulic systems. The flow dynamics of these systems are governed by *shallow water equations* (SWE) which are nonlinear, hyperbolic PDEs, also known as the Saint-Venant equations [3]. In many practical applications, these equations are linearized around a nominal flow. If the linearization is done about a gradually varied steady state profile, the coefficients of the

linearized PDE are spatially varying [4]. These coefficients are nonlinear functions of the physical system parameters such as the canal geometry, the friction factor as well as the steady state boundary conditions. An accurate knowledge of these physical parameters is essential for understanding the flow dynamics in natural river systems [5] and for efficiently controlling the canal networks [6],[7].

However, in most natural river systems, these parameters are unknown and have to be estimated from the flow variables measured by (fixed) Eulerian sensors [8] or (moving) Lagrangian sensors [9]. It then becomes important to investigate techniques for accurate identification of the physical parameters of open-channel hydraulic systems. In this article, the problem of estimating the parameters of a linearized SWE subjected to periodic forcing is considered. This setting can model the effect of tidal excitations on the flow dynamics of long river reaches located much upstream of the river-ocean confluence. In the current setting, the data of the problem is the flow variables that are monitored at the upstream and downstream ends as well as at selected intermediate locations. The parameters to be estimated are: the canal width, the bed slope, the roughness coefficient and the steady state upstream and downstream boundary conditions. The problem is to find the parameter values such that the estimated linear SWE describes the measured data as *best* as possible. The spatial dependence of these parameters is not considered in the current work.

A common approach to achieve this objective is to choose the parameter values that minimize the output least squares error functional between the model predictions and the measured data [10]. However, this formulation involves minimization of a cost function, subjected to PDE constraints and it may be difficult to solve in a numerically efficient manner [8]. In this article, tools from the frequency domain modeling of linear PDEs are used to convert the PDE constrained minimization problem to one without any PDE constraints. By modal analysis, the input data is expressed in terms of a small number of Fourier modes. The spatially dependent transfer matrix relating the input variables to the output variables is then used to obtain a parameterized *prediction* of the output response for the chosen set of modal inputs. The optimal parameters can be obtained by minimizing the squared deviations of the output predictions from the measured data. This minimization problem is considerably easier to solve in comparison to the original PDE constrained minimization problem. This is the main contribution of the article.

The article is organized as follows: Section II introduces the

This work is supported by NSF grants CCR-0225610 and CNS-0615299.

[‡] Department of Civil and Environmental Engineering, UC Berkeley, CA, USA – {amins, bayen}@berkeley.edu

[†] Cemagref, UMR G-EAU, B.P. 5095, 34196 Montpellier Cedex 5, France – {simon.munier, xavier.litrico}@cemagref.fr

^{*} SupAgro - GR, UMR G-EAU, Montpellier, France – {belaud}@ensam.inra.fr

linearized SWE and defines the associated forward simulation and the parameter identification problems. The parameter identification problem is stated as a PDE constrained minimization problem. Section III uses a frequency domain modeling techniques to obtain a spatially dependent transfer matrix relating the input flow variables to the output flow variables. Section IV proposes a method based on the use of modal decomposition of inputs and the input-output transfer matrix to obtain a simpler formulation of the parameter identification problem. In Section V, the proposed method is applied to a river reach in the Sacramento–San-Joaquin Delta for which system parameters and steady state boundary conditions are estimated using the measured flow variables at the upstream and downstream end of the river reach. The validity of results is confirmed by comparing the flows predicted by the estimated model with the flows measured at an intermediate location. Conclusion and the scope for future work is presented in Section VI.

II. SYSTEM MODEL AND PROBLEM STATEMENT

A. The Saint-Venant Model

The Saint-Venant equations are quasi-linear hyperbolic PDEs that describe the dynamics of one-dimensional flow in open-channel hydraulic systems [11],[3]. For a rectangular cross-section, these equations are given by:

$$TY_t + Q_x = 0 \quad (1)$$

$$Q_t + \left(\frac{Q^2}{TY} + \frac{gTY^2}{2} \right)_x + gTY(S_f - S_b) = 0 \quad (2)$$

for $(x, t) \in (0, X) \times \mathbb{R}^+$, where X the river reach m , $Q(x, t)$ the discharge (m^3/s) across cross-section $A(x, t) = TY(x, t)$, $Y(x, t)$ the stage or water-depth (m), T the free surface width (m) which is constant for rectangular cross-section, $S_f(x, t)$ the friction slope (m/m), S_b the bed slope m/m , g the gravitational acceleration (m/s^2). Also, $V(x, t)$ the average velocity (m/s) in the cross-section A defined by $V = \bar{Q}/A$ and $P(x, t)$ the wetted perimeter (m) defined by $P(x, t) = T + 2Y(x, t)$. The boundary conditions are $Q(0, t) = Q_0(t)$ and $Y(X, t) = Y_0(t)$. The initial conditions are given by $Q(x, 0)$ and $Y(x, 0)$ for $x \in [0, X]$. The friction slope is empirically modeled by the Manning-Strickler's formula

$$S_f = \frac{Q^2 n^2 (T + 2Y)^{4/3}}{(TY)^{10/3}} \quad (3)$$

with n the Manning's roughness coefficient ($sm^{-1/3}$). Under constant boundary conditions, equations (1,2) admit a *steady state solution*. Let the flow variables corresponding to the steady state condition be denoted by $Q_0(x)$, $Y_0(x)$ etc. where $x \in [0, X]$. The steady state equations are given by

$$\frac{dQ_0(x)}{dx} = 0 \quad (4)$$

$$\frac{dY_0(x)}{dx} = \frac{S_b - S_{f0}}{1 - F_0(x)^2} \quad (5)$$

with $C_0 = \sqrt{gY_0}$ the wave celerity, $F_0 = V_0/C_0$ the Froude number and $V_0 = Q_0/A_0$ the steady state velocity. While $Q_0(x) = Q_0 = Q_X$ by the first equation, the second equation is solved for $Y_0(x)$ with boundary condition in terms of downstream elevation $Y_0(X)$. In this article, we assume the flow to be *sub-critical*, i.e., $F_0 < 1$.

B. Linearized Saint-Venant Model

Following [4], equations (1),(2) can be linearized around the steady state flow variables $Q_0(x)$ and $Y_0(x)$. The linearized equations for perturbed flow variables $q = Q(x, t) - Q_0(x)$ and $y = Y(x, t) - Y_0(x)$ are:

$$T_0 y_t + q_x = 0 \quad (6)$$

$$q_t + 2V_0(x)q_x - \beta_0(x)q + \alpha_0(x)y_x - \gamma_0(x)y = 0 \quad (7)$$

with $\alpha_0(x)$, $\beta_0(x)$ and $\gamma_0(x)$ given by:

$$\alpha_0 = (C_0^2 - V_0^2)T_0 \quad (8)$$

$$\beta_0 = -\frac{2g}{V_0} \left(S_b - \frac{dY_0}{dx} \right) \quad (9)$$

$$\gamma_0 = gT_0 \left[(1 + \kappa_0)S_b - (1 + \kappa_0 - (\kappa_0 - 2)F_0^2) \frac{dY_0}{dx} \right] \quad (10)$$

with $\kappa_0 = 7/3 - 8Y_0/(3(2Y_0 + T))$. In the above equations, to emphasize the free surface width T is uniform, it is denoted as T_0 and the dependence on x is omitted for readability. The upstream and downstream boundary conditions are respectively given by the upstream discharge perturbation $q(0, t)$ and the downstream stage perturbation $y(X, t)$. The initial conditions are given by $y(x, 0) = 0$ and $q(x, 0) = 0$ for all $x \in [0, X]$. The linearized Saint-Venant model (6,7) can be written in the following form:

$$u_t = \mathcal{A}(x)u \quad (11)$$

where u is the two-dimensional vector function $u(x, t) = (u_1(x, t), u_2(x, t))^T := (q(x, t), y(x, t))^T$ defined on $(x, t) \in \mathbb{R}^+$, and $\mathcal{A}(x)$ denotes the linear operator given by:

$$\mathcal{A}(x) = - \left(\begin{array}{cc} 2V_0(x) & \alpha_0(x) \\ \frac{1}{T_0} & 0 \end{array} \right) \frac{\partial}{\partial x} + \left(\begin{array}{cc} \beta_0(x) & \gamma_0(x) \\ 0 & 0 \end{array} \right) \quad (12)$$

The boundary conditions of (11) are given by

$$u_1(0, t) \text{ and } u_2(X, t) \quad (13)$$

and initial conditions given by

$$u(x, 0) = 0, \forall x \in [0, X] \quad (14)$$

C. Problem Statement

In this article, the boundary conditions $u_1(0, t) = q(0, t)$ and $u_2(X, t) = y(X, t)$ are the *measured input variables*, the downstream discharge perturbation $u_1(X, t) = q(X, t)$ and the upstream stage perturbation $u_2(0, t) = y(0, t)$ are the *measured output variables*; the measured input and output variables are assumed to be known from a reference time 0 to a final time τ . Thus, for the linear PDE system (11), the measured data is the vector function $u(x, t)$ recorded at $x = 0$ and $x = X$. The properties of the measured data depend on a variety of factors such as the environment, sensor characteristics, etc. In addition, it is assumed that $u(x, 0) = 0$ for all $x \in [0, X]$.

The Manning roughness coefficient n , the free surface width T_0 , the bed slope S_b , the steady state discharge Q_0 and the steady state downstream stage $Y_0(X)$ are the *unknown*

parameters of the system (11). We define the parameter vector $\theta := (T_0, S_b, n, Q_0, Y_0(X))^T$ that ranges over the set:

$$\mathcal{D}_{\mathcal{A}} := [\underline{T}_0, \overline{T}_0] \times [\underline{S}_b, \overline{S}_b] \times [\underline{n}, \overline{n}] \times [\underline{Q}_0, \overline{Q}_0] \times [\underline{Y}_0(X), \overline{Y}_0(X)] \quad (15)$$

The linear operator $\mathcal{A}(x)$ can be considered to be parameterized by θ that ranges over the parameter set $\mathcal{D}_{\mathcal{A}}$. We define the set of all linear operators allowed by $\mathcal{D}_{\mathcal{A}}$ as $\mathbf{A}(x)$ which is given by:

$$\mathbf{A}(x) := \{\mathcal{A}(\theta; x) | \theta \in \mathcal{D}_{\mathcal{A}}\} \quad (16)$$

where, $\mathcal{A}(\theta; x)$ encodes the linear operator (12) for a given θ . To emphasize the dependence on θ of the linearized Saint-Venant model, (11) is written as:

$$u_t = \mathcal{A}(\theta; x)u \quad (17)$$

We now define the forward and the inverse problems.

Definition 1: (Forward simulation). For a given θ , find u satisfying: (17) with boundary conditions (13) and initial conditions (14).

Definition 2: (Parameter identification). Given the set of linear operators $\mathbf{A}(x)$, recover the parameter set θ that *optimally* fits the model, (17) with boundary conditions (13) and initial conditions (14), to the measured data $u(X, t)$ and $u(0, t)$ recorded for all $t \in [0, \tau]$.

Often, the forward simulation problem is simply called the *forward problem* and the parameter identification problem is called the *inverse problem*. The identified parameter vector in the problem will be denoted $\hat{\theta}$. In the definition of *inverse problem*, the optimality of the identified parameter vector $\hat{\theta}$ with respect to the given data needs to be defined. It should be noted that once the parameter identification problem is solved for $\hat{\theta}$, the forward simulation problem can be solved to obtain the *predicted output variables*: $\hat{u}_1(X, t|\theta) = \hat{q}(X, t|\theta)$ and $\hat{u}_2(0, t|\theta) = \hat{y}(0, t|\theta)$. The notation $\hat{u}_1(X, t|\theta)$ indicates the prediction of $u_1(X, t)$ by the PDE model under appropriate initial and boundary conditions and knowledge of the parameter vector θ .

We define a scalar valued cost function as:

$$\begin{aligned} \mathcal{J}(\theta; \tau; u(0, \cdot), u(X, \cdot)) &= \int_0^\tau \frac{w_1}{u_{1, \text{norm}}^2} (u_1(X, t) - \hat{u}_1(X, t|\theta))^2 dt \\ &+ \int_0^\tau \frac{w_2}{u_{2, \text{norm}}^2} (u_2(0, t) - \hat{u}_2(0, t|\theta))^2 dt \end{aligned} \quad (18)$$

where, w_1 and w_2 denote the weighing factors for the cost function and $u_{1, \text{norm}}$ and $u_{2, \text{norm}}$ denote normalizing coefficients of the cost function. Here, it is assumed that, the data $u(0, t)$ and $u(X, t)$ is recorded for $t \in [0, \tau]$.

It is important to note that implicit in equation (18) is the requirement that for any given θ and τ , the evaluation of the cost function would require solving the forward problem: Solve (17) with boundary conditions (13) and initial conditions (14). If $\phi(x, t|\theta)$, $(x, t) \in [0, X] \times [0, \tau]$ is the solution of the forward problem, the predictions can be obtained by assigning $\hat{u}_1(X, t|\theta) = \phi(X, t|\theta)$ and $\hat{u}_2(0, t|\theta) = \phi(0, t|\theta)$

for $t \in [0, \tau]$. Thus, the parameter identification problem can be stated as follows:

Problem 1: Solve the minimization problem:

$$\hat{\theta} = \arg \min_{\theta \in \mathcal{D}_{\mathcal{A}}} \mathcal{J}(\theta; \tau; u(0, \cdot), u(X, \cdot)) \quad (19)$$

with $\mathcal{J}(\theta; \tau; u(0, \cdot), u(X, \cdot))$ given by (18) and subject to the PDE constraint: $\hat{u}_1(X, t|\theta) = \phi(X, t|\theta)$ and $\hat{u}_2(0, t|\theta) = \phi(0, t|\theta)$, where $\phi(x, t|\theta)$ is the solution of the forward problem: (17) with boundary conditions (13) and initial conditions (14).

The resulting estimate of the linearized Saint-Venant system is given by:

$$u_t = \mathcal{A}(\hat{\theta}; x)u \quad (20)$$

with boundary conditions $u_1(0, t)$ and $u_2(X, t)$ and zero initial conditions.

III. SAINT-VENANT DISTRIBUTED TRANSFER MATRIX

This section is concerned with the frequency domain modeling of the linearized Saint-Venant equations.

A. Uniform flow case for upstream flow variables as boundary conditions

For the case of uniform flow, the application of the Laplace transform to the linear partial PDE system (11) leads to the *ordinary differential equation* (ODE) in variable x , with the Laplace variable s (see [4] for details). Solving this ODE with boundary conditions $u_1(0, s)$ and $u_2(0, s)$, leads to the open-loop distributed transfer matrix for the case of uniform flow, $\mathcal{G}^v(x, s) = (g_{ij}^v(x, s))$, relating the flow variables at any point x of the river reach $u(x, s)$ to the upstream flow variables $u(0, s)$:

$$\begin{pmatrix} u_1(x, s) \\ u_2(x, s) \end{pmatrix} = \begin{pmatrix} g_{11}^v(x, s) & g_{12}^v(x, s) \\ g_{21}^v(x, s) & g_{22}^v(x, s) \end{pmatrix} \begin{pmatrix} u_1(0, s) \\ u_2(0, s) \end{pmatrix} \quad (21)$$

with

$$\begin{aligned} g_{11}^v(x, s) &= \frac{\lambda_2 e^{\lambda_1 x} - \lambda_1 e^{\lambda_2 x}}{\lambda_2 - \lambda_1}, \quad g_{12}^v(x, s) = -T_0 s \frac{e^{\lambda_2 x} - e^{\lambda_1 x}}{\lambda_2 - \lambda_1}, \\ g_{21}^v(x, s) &= \frac{\lambda_1 \lambda_2}{T_0 s} \frac{e^{\lambda_2 x} - e^{\lambda_1 x}}{\lambda_2 - \lambda_1} \quad \text{and} \quad g_{22}^v(x, s) = \frac{\lambda_2 e^{\lambda_2 x} - \lambda_1 e^{\lambda_1 x}}{\lambda_2 - \lambda_1}. \end{aligned}$$

Here, λ_1 and λ_2 are the eigenvalues of the ODE system, and are given by:

$$\begin{aligned} \lambda_i(s) &= \frac{2T_0 V_0 s + \gamma_0}{2\alpha_0} \\ &+ (-1)^i \frac{\sqrt{4C_0^2 T_0^2 s^2 + 4T_0(V_0 \gamma_0 - \alpha_0 \beta_0)s + \gamma_0^2}}{2\alpha_0} \end{aligned} \quad (22)$$

B. Uniform flow case for input variables as boundary conditions

Equation (21) can be modified to the case when the boundary conditions are $u_1(0, s)$ and $u_2(X, s)$. The distributed transfer matrix $\mathcal{G}^u(x, X, s) = (g_{ij}^u(x, X, s))$ relating the flow variables at any point x of the river reach $u(x, s)$ to the measured input variables $u_1(0, s)$ and $u_2(X, s)$ (see Section II-C) of the river reach is given by the equation:

$$\begin{pmatrix} u_1(x, s) \\ u_2(x, s) \end{pmatrix} = \begin{pmatrix} g_{11}^u(x, X, s) & g_{12}^u(x, X, s) \\ g_{21}^u(x, X, s) & g_{22}^u(x, X, s) \end{pmatrix} \begin{pmatrix} u_1(0, s) \\ u_2(X, s) \end{pmatrix} \quad (23)$$

with $g_{11}^u(x, X, s) = \frac{\lambda_2 e^{\lambda_1 x + \lambda_2 X} - \lambda_1 e^{\lambda_2 x + \lambda_1 X}}{\lambda_2 e^{\lambda_2 X} - \lambda_1 e^{\lambda_1 X}}$, $g_{12}^u(x, X, s) = -T_0 s \frac{e^{\lambda_2 x} - e^{\lambda_1 x}}{\lambda_2 e^{\lambda_2 X} - \lambda_1 e^{\lambda_1 X}}$, $g_{21}^u(x, X, s) = \frac{\lambda_1 \lambda_2}{T_0 s} \frac{e^{\lambda_2 x + \lambda_1 X} - e^{\lambda_1 x + \lambda_2 X}}{\lambda_2 e^{\lambda_2 X} - \lambda_1 e^{\lambda_1 X}}$ and $g_{22}^u(x, X, s) = \frac{\lambda_2 e^{\lambda_2 x} - \lambda_1 e^{\lambda_1 x}}{\lambda_2 e^{\lambda_2 X} - \lambda_1 e^{\lambda_1 X}}$ where, λ_1 and λ_2 are given by (22).

C. Non-uniform case using backwater approximation

Following the method used by [12], the backwater curve defined by equation (5) is approximated by two straight lines as represented in Figure 1. The river reach is then decomposed into two parts: a uniform part and a backwater part. The abscissa of the limit between the parts is denoted x_1 . Let $x_u = x$ denote the location in the uniform part, $x_b = x - x_1$ denote the location in the backwater part. $X_u = x_1$ denote the length of the uniform part and $X_b = X - x_1$ denote the length of the backwater part. Let $\mathcal{G}^u(x_u, X_u, s)$ and $\mathcal{G}^b(x_b, X_b, s)$ respectively denote the transfer matrices for the uniform and the backwater parts. These matrices have the same form as the transfer matrix in the uniform case (see equation (23)). The transfer matrix for the non-uniform case is denoted as $\mathcal{G}^n(x, X, s) = (g_{ij}^n(x, X, s))$ with

$$\begin{pmatrix} u_1(x, s) \\ u_2(x, s) \end{pmatrix} = \begin{pmatrix} g_{11}^n(x, X, s) & g_{12}^n(x, X, s) \\ g_{21}^n(x, X, s) & g_{22}^n(x, X, s) \end{pmatrix} \begin{pmatrix} u_1(0, s) \\ u_2(X, s) \end{pmatrix} \quad (24)$$

The entries of the transfer matrix for the non-uniform case are given by:

- $x < x_1$:

$$\begin{aligned} g_{11}^n(x, X, s) &= g_{11}^u(x, x_1, s) \\ &+ \frac{g_{12}^u(x, x_1, s)g_{11}^u(x_1, x_1, s)g_{21}^b(0, X_b, s)}{1 - g_{12}^u(x_1, x_1, s)g_{21}^b(0, X_b, s)} \\ g_{12}^n(x, X, s) &= \frac{g_{12}^u(x, x_1, s)g_{22}^b(0, X_b, s)}{1 - g_{12}^u(x_1, x_1, s)g_{21}^b(0, X_b, s)} \\ g_{21}^n(x, X, s) &= g_{21}^u(x, x_1, s) \\ &+ \frac{g_{22}^u(x, x_1, s)g_{11}^u(x_1, x_1, s)g_{21}^b(0, X_b, s)}{1 - g_{12}^u(x_1, x_1, s)g_{21}^b(0, X_b, s)} \\ g_{22}^n(x, X, s) &= \frac{g_{22}^u(x, x_1, s)g_{22}^b(0, X_b, s)}{1 - g_{12}^u(x_1, x_1, s)g_{21}^b(0, X_b, s)} \end{aligned}$$

- $x > x_1$:

$$\begin{aligned} g_{11}^n(x, X, s) &= \frac{g_{11}^b(x_b, X_b, s)g_{11}^u(x_1, x_1, s)}{1 - g_{12}^u(x_1, x_1, s)g_{21}^b(0, X_b, s)} \\ g_{12}^n(x, X, s) &= g_{12}^b(x_b, X_b, s) \\ &+ \frac{g_{11}^b(x_b, X_b, s)g_{12}^u(x_1, x_1, s)g_{22}^b(0, X_b, s)}{1 - g_{12}^u(x_1, x_1, s)g_{21}^b(0, X_b, s)} \\ g_{21}^n(x, X, s) &= \frac{g_{21}^b(x_b, X_b, s)g_{11}^u(x_1, x_1, s)}{1 - g_{12}^u(x_1, x_1, s)g_{21}^b(0, X_b, s)} \\ g_{22}^n(x, X, s) &= g_{22}^b(x_b, X_b, s) \\ &+ \frac{g_{21}^b(x_b, X_b, s)g_{12}^u(x_1, x_1, s)g_{22}^b(0, X_b, s)}{1 - g_{12}^u(x_1, x_1, s)g_{21}^b(0, X_b, s)} \end{aligned}$$

- $x = x_1$:

$$\begin{aligned} g_{11}^n(x, X, s) &= \frac{g_{11}^u(x_1, x_1, s)}{1 - g_{12}^u(x_1, x_1, s)g_{21}^b(0, X_b, s)} \\ g_{12}^n(x, X, s) &= \frac{g_{12}^u(x_1, x_1, s)g_{22}^b(0, X_b, s)}{1 - g_{12}^u(x_1, x_1, s)g_{21}^b(0, X_b, s)} \\ g_{21}^n(x, X, s) &= \frac{g_{21}^b(0, X_b, s)g_{11}^u(x_1, x_1, s)}{1 - g_{12}^u(x_1, x_1, s)g_{21}^b(0, X_b, s)} \\ g_{22}^n(x, X, s) &= \frac{g_{22}^b(0, X_b, s)}{1 - g_{12}^u(x_1, x_1, s)g_{21}^b(0, X_b, s)} \end{aligned}$$

In the following sections, the notation $\mathcal{G}^n(\theta; x, X, s)$ will be used to emphasize the non-uniform transfer matrix for parameter vector θ .

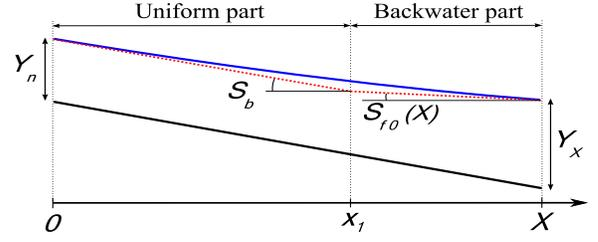


Fig. 1. Backwater curve approximation

IV. PROPOSED APPROACH

This section uses the input-output transfer matrix $\mathcal{G}^n(\theta; x, X, s)$ in Section III-C to obtain a more direct formulation of the parameter estimation problem (refer to Problem 1) in which the cost function explicitly incorporates the constraint. The main idea behind the proposed approach is to decompose the input variables $u_1(0, t)$ and $u_2(X, t)$ into a finite sum of dominant oscillatory modes. In the case of a river reach influenced by the ocean at the downstream end, these modes can be thought as the principle modes of excitation produced by the tidal forcing. Under the assumption of N most dominant oscillatory modes, the input variables can be expressed as:

$$u_1(0, t) \approx \sum_{k=0}^N \left[d_k^{(1,0)} e^{j\omega_k t} + \overline{d_k^{(1,0)}} e^{-j\omega_k t} \right] \quad (25)$$

$$u_2(X, t) \approx \sum_{k=0}^N \left[d_k^{(2,X)} e^{j\omega_k t} + \overline{d_k^{(2,X)}} e^{-j\omega_k t} \right] \quad (26)$$

where $d_k^{(1,0)}$ and $d_k^{(2,X)}$, $k = 0, \dots, N$, are respectively the Fourier coefficients of the spectral decomposition of $u_1(0, t)$ and $u_2(X, t)$. ω_k is the set of frequencies used for the modal decomposition.

Now, the non-uniform transfer matrix $\mathcal{G}^n(\theta; x, X, s)$ (see (24)) can be used to compute the output predictions $\hat{u}_1(X, t|\theta)$ and $\hat{u}_2(0, t|\theta)$ that go in the definition of the cost function:

$$\hat{u}_1(X, t|\theta) = \sum_{k=0}^N \left[\alpha_k^{(1,X)}(\theta) e^{j\omega_k t} + \overline{\alpha_k^{(1,X)}(\theta)} e^{-j\omega_k t} \right] \quad (27)$$

$$\hat{u}_2(0, t|\theta) = \sum_{k=0}^N \left[\alpha_k^{(2,0)}(\theta) e^{j\omega_k t} + \overline{\alpha_k^{(2,0)}(\theta)} e^{-j\omega_k t} \right] \quad (28)$$

with coefficients in the equations given by

$$\begin{aligned} \alpha_k^{(1,X)}(\theta) &= d_k^{(1,0)} g_{11}^n(\theta; X, X, j\omega_k) + d_k^{(2,X)} g_{12}^n(\theta; X, X, j\omega_k) \\ \overline{\alpha_k^{(1,X)}(\theta)} &= \overline{d_k^{(1,0)}} g_{11}^n(\theta; X, X, -j\omega_k) + \overline{d_k^{(2,X)}} g_{12}^n(\theta; X, X, -j\omega_k) \\ \alpha_k^{(2,0)}(\theta) &= d_k^{(1,0)} g_{21}^n(\theta; 0, X, j\omega_k) + d_k^{(2,X)} g_{22}^n(\theta; 0, X, j\omega_k) \\ \overline{\alpha_k^{(2,0)}(\theta)} &= \overline{d_k^{(1,0)}} g_{21}^n(\theta; 0, X, -j\omega_k) + \overline{d_k^{(2,X)}} g_{22}^n(\theta; 0, X, -j\omega_k) \end{aligned}$$

Note that the number of modes N in equations (25,26) and (27,28) is the same because the PDE is non-dispersive. It should be noted that

$$g_{ij}^n(\theta; x, X, -j\omega_k) = \overline{g_{ij}^n(\theta; x, X, j\omega_k)}.$$

Similarly, the measured output variables $u_1(X, t)$ and

$u_2(0, t)$ can be expressed as the infinite sum of response modes

$$u_1(X, t) = \sum_{k=0}^{\infty} \left[\alpha_k^{(1,X)} e^{j\omega_k t} + \overline{\alpha_k^{(1,X)}} e^{-j\omega_k t} \right] \quad (29)$$

$$u_2(0, t) = \sum_{k=0}^{\infty} \left[\alpha_k^{(2,0)} e^{j\omega_k t} + \overline{\alpha_k^{(2,0)}} e^{-j\omega_k t} \right] \quad (30)$$

Substituting the the expressions in equations (27,28,29,30) in the expression for cost function (18), we obtain:

$$\begin{aligned} & \mathcal{J}(\theta; \tau; u(0, \cdot), u(X, \cdot)) \\ & \approx \hat{\mathcal{J}} \left(\theta; N; \left\{ d_k^{(1,0)}, d_k^{(2,X)} \right\}_{k=0}^N, \left\{ \alpha_k^{(1,X)}, d_k^{(2,0)} \right\}_{k=0}^{\infty} \right) \\ & = 2\tau \sum_{k=0}^N \left(\frac{w_1}{u_{1,\text{norm}}^2} \left| \alpha_k^{(1,X)}(\theta) - \alpha_k^{(1,X)} \right|^2 \right) \\ & + 2\tau \sum_{k=0}^N \left(\frac{w_2}{u_{2,\text{norm}}^2} \left| \alpha_k^{(2,0)}(\theta) - \alpha_k^{(2,0)} \right|^2 \right) \\ & + 2\tau \sum_{k=N+1}^{\infty} \left(\frac{w_1}{u_{1,\text{norm}}^2} \left| \alpha_k^{(1,X)} \right|^2 + \frac{w_2}{u_{2,\text{norm}}^2} \left| \alpha_k^{(2,0)} \right|^2 \right) \quad (31) \end{aligned}$$

where, the integration has been carried explicitly over $[0, \tau]$, with τ multiple of the smallest period of the N most dominant modes. Renormalizing for optimization purposes, the modified cost function $\tilde{\mathcal{J}}$ is defined as:

$$\begin{aligned} & 2\tau \sum_{k=0}^N \left[w_1 \left| \frac{\alpha_k^{(1,X)}(\theta) - \alpha_k^{(1,X)}}{\alpha_{k,n}^{(1,X)}} \right|^2 \right] \\ & + 2\tau \sum_{k=0}^N \left[w_2 \left| \frac{\alpha_k^{(2,0)}(\theta) - \alpha_k^{(2,0)}}{\alpha_{k,n}^{(2,0)}} \right|^2 \right] \\ & + 2\tau \sum_{k=N+1}^{\infty} \left[w_1 \left| \frac{\alpha_k^{1,X}}{\alpha_{k,n}^{(1,X)}} \right|^2 + w_2 \left| \frac{\alpha_k^{2,0}}{\alpha_{k,n}^{(2,0)}} \right|^2 \right] \quad (32) \end{aligned}$$

with $\alpha_{k,n}^{(1,X)}$, $\alpha_{k,n}^{(2,0)}$ the normalizing coefficients of the Fourier coefficients.¹

It can be noted that the the third term in the expression of cost function in (32) does not depend on parameter vector θ and hence, does not affect the minimization of the cost function. Therefore, the parameter estimation problem can be expressed as:

$$\hat{\theta} = \arg \min_{\theta \in \mathcal{D}_A} \tilde{\mathcal{J}} \left(\theta; N; \left\{ d_k^{(1,0)}, d_k^{(2,X)} \right\}_{k=0}^N, \left\{ \alpha_k^{(1,X)}, \alpha_k^{(2,0)} \right\}_{k=0}^N \right) \quad (33)$$

with

$$\begin{aligned} & \tilde{\mathcal{J}} \left(\theta; N; \left\{ d_k^{(1,0)}, d_k^{(2,X)} \right\}_{k=0}^N, \left\{ \alpha_k^{(1,X)}, \alpha_k^{(2,0)} \right\}_{k=0}^N \right) \\ & = 2\tau \sum_{k=0}^N \left[w_1 \left| \frac{\alpha_k^{(1,X)}(\theta) - \alpha_k^{(1,X)}}{\alpha_{k,n}^{(1,X)}} \right|^2 \right. \\ & \left. + w_2 \left| \frac{\alpha_k^{(2,0)}(\theta) - \alpha_k^{(2,0)}}{\alpha_{k,n}^{(2,0)}} \right|^2 \right] \quad (34) \end{aligned}$$

This problem is now an unconstrained optimization problem and can be solved using standard non-linear programming.

¹Note that choosing the same normalizing coefficients for all frequencies give more weight to the dominant frequencies, while choosing the coefficients of the response output modes as the normalizing coefficients give same weight to all the selected dominant frequencies.

V. CASE STUDY: THE SACRAMENTO DELTA

In this section, we apply the proposed approach for estimating parameters for a river reach in the Sacramento-San Joaquin Delta.

A. Parameter identification problem for a river reach

The Sacramento-San Joaquin Delta in California, USA, is a complex network of over 1150 km of tidally-influenced channels and sloughs. The San Joaquin River, with a length of 530 km, is the second-longest river in the Delta area. The field of interest for our experiment is the San Joaquin River reach between DWR and USGS stations (*SJL* and *SJG*), as shown in Figure 2. The available data is the discharge perturbation, the stage perturbation for the stations *SJL*, *SJG* and the stage perturbation at *BDT*. The direction of the mean flow is from *SJL* to *SJG*. Measurements are available at every 900 s. The data was collected between 11/16/2006 and 12/17/2006.

This study makes the following simplifying assumptions:

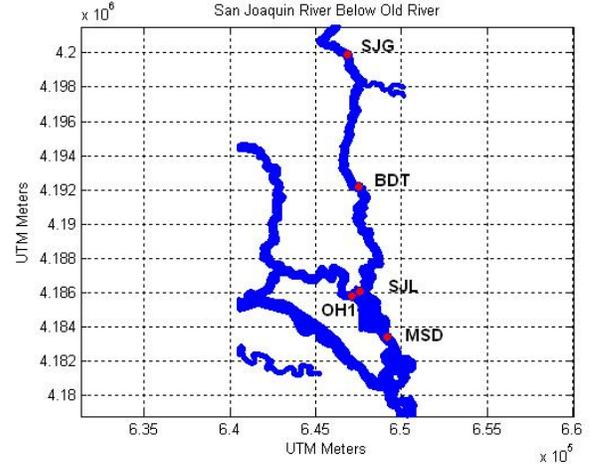


Fig. 2. DWR satellite stations along San Joaquin River.

the flow is one dimensional; the wavelength of tidal forcing is long relative to the water stage; lateral and vertical accelerations are negligible; pressure distribution is hydrostatic; the channel geometry is fixed and can be averaged by a rectangular cross-section; the bed slope is small and water surface across any cross-section is horizontal.

Consider the station *SJL* to be the origin and the station *SJG* located at abscissa X from the origin. The input variables are the discharge perturbation at *SJL* and the stage perturbation at *SJG*. The output variables are the discharge perturbation at *SJG* and the stage perturbation at *SJL*. The parameter estimation problem is to estimate the average free surface width T_0 , the average bottom slope S_b , the average Manning's coefficient n , the average discharge upstream Q_0 and the average downstream stage Y_X .

B. Spectral analysis

Figure 3 shows the spectral analysis for the total stage at station *SJL*. The power spectrum is cutoff at 0.02dB/Hz

to determine the 27 dominant frequencies. The figure also compares the measured stage and the stage generated from the first 27 modes. The results indicate that 27 modes are enough to capture the signal; the amplitude at 0 Hz is actually the nominal stage. There are three dominant tidal frequencies in the system: $\omega_1 = 0.0001407 \text{ s}^{-1}$ (or period 12.4 *hrs*), corresponding to the M2 tide generated by the Moon; $\omega_2 = 0.0000727 \text{ s}^{-1}$ (or period 24 *hrs*) corresponding to the K1 tide generated by the Sun and a $\omega_3 = 0.000068 \text{ s}^{-1}$ (or period 25 *hrs*) tide. Similar arguments hold for other

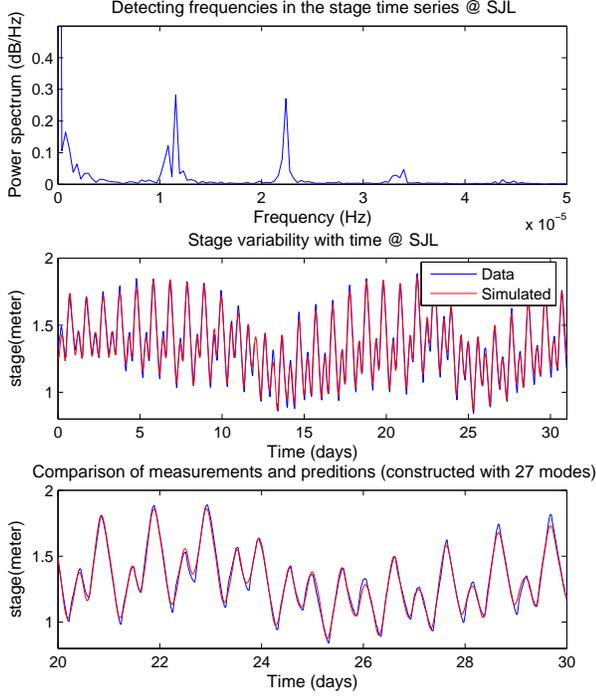


Fig. 3. Stage Analysis at SJL Station.

measured variables.

C. Parameter identification

This study assumes $\alpha_{k,n}^{(1,X)} = \alpha_k^{(1,X)}$, $\alpha_{k,n}^{(2,0)} = \alpha_k^{(2,0)}$ so that each significant frequency has the same weight. The weighing factors w_1, w_2 are chosen to be 1. The constrained optimization function in MATLAB is used to identify the parameters listed in Table I. This optimization process converges quickly leading to the desired estimates. In this case, the value of optimal cost function is equal to $\tilde{J} = 0.093$. The values of T_0 , S_b , and n are acceptable.

Q_0	Y_X	T_0	S_b	n
$11.5 \text{ m}^3\text{s}^{-1}$	4.04 m	47.00 m	0.0002	$0.048 \text{ m}^{-1/3}\text{s}$

TABLE I
IDENTIFIED PARAMETERS FOR SAN JOAQUIN RIVER.

The estimated values of Q_0 and Y_X are not as good as the others, for the expected values are respectively $7.34 \text{ m}^3/\text{s}$ and 10.0 m . This can be partly explained by recalling that

the transfer matrix for the non-uniform flow $\mathcal{G}^n(\theta; x, X, s)$ was derived using the two-pool approximation (see Section III-C). A further improvement in the non-uniform transfer matrix might improve accuracy of the predicted steady state boundary conditions.

The comparison of the predicted and measured outputs is shown in Figure 4 (that is, the stage perturbation at *SJL* and the discharge perturbation at *SJG*). It can be observed that the estimated model accurately predicts the measured output values.

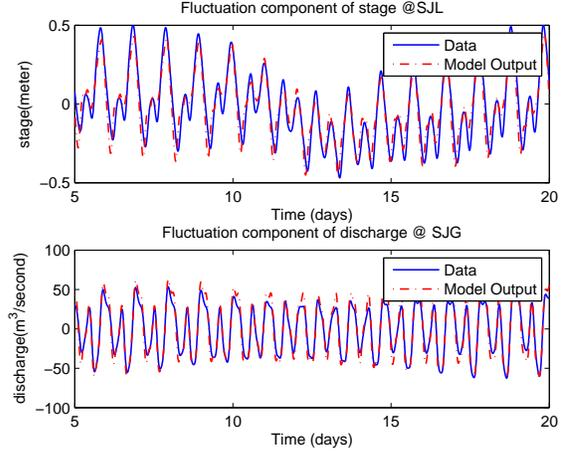


Fig. 4. Parameter Identification: model output v.s. measurement.

D. Sensitivity

The graphs in figure (5) present the variations of the cost function \tilde{J} with respect to each parameter. For each graph, one parameter changes, while all others remain constant at the values corresponding to the minimum of \tilde{J} . A flat curve signifies that any other value of the parameter would lead to the same value of \tilde{J} . In this case, the minimum on each graph is clearly defined. The cost function appears to be less sensitive to a variation of the slope. This may be due to the fact that the flow dynamics of the channel is dominated by the downstream water depth (backwater part). In that case, the slope has small influence on the flow dynamics. Thus, it can be concluded that the objective function and the model are sensitive enough to successfully evaluate the parameters.

E. Validation

The stage time series at BDT station, along with the given parameters in Table I, are used to validate the model. From Figure 6, it can be concluded that the model output gives an accurate prediction of the validation data.

F. Predictability

The data collected between 12/18/2006 and 2/18/2007 were used to further test the predictive capability of the model, with the identified parameters given in Table I. Following the steps described in the previous sections, the stage outputs at BDT station have been predicted, using the

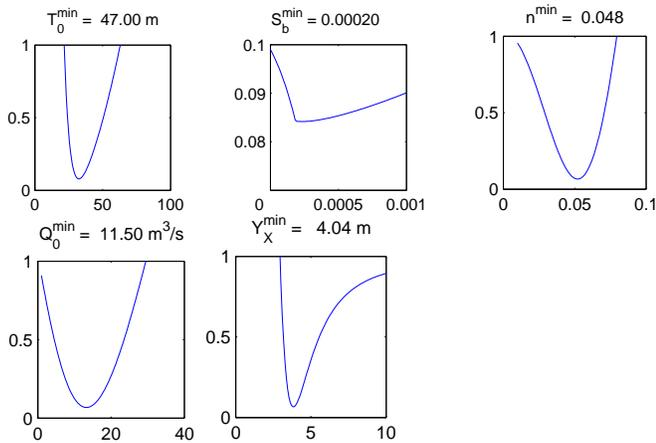


Fig. 5. Sensitivity analysis for the application case.

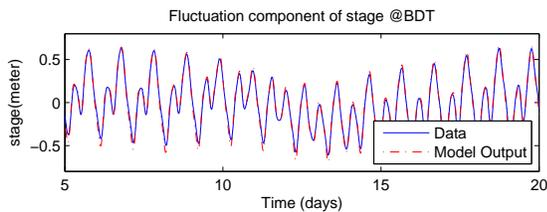


Fig. 6. Model Validation: model output v.s. measurement.

discharge data at SJL station and the stage data at SJG station during the time interval. Comparing with the observed stage data, it is clear that the model successfully characterizes the flow, with a good reflection of the stage fluctuation tendency in the time domain (Figure 7). The cost function in this case is equal to $\tilde{J} = 0.044$ which is of the same order as the optimal cost function for the parameter identification stage (refer to Section V-C).

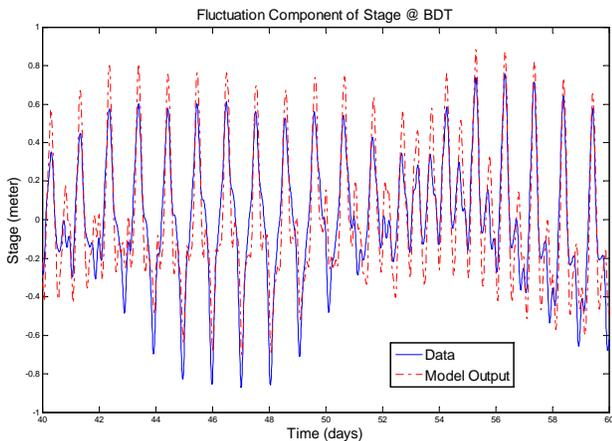


Fig. 7. Model Predictability during 12/18/2006 and 2/18/2007: model output v.s. measurement.

VI. CONCLUSION

This article proposes a new approach to solve a parameter identification problem for linear hyperbolic partial differential equations that are subjected to periodic

forcing. Using frequency domain modeling techniques such as modal decomposition and approximation of transfer matrix for the non-uniform steady state case by composing two (or more) transfer matrices for the uniform case, the output response can be expressed in terms of the spectral coefficients of the input excitation and the transfer matrix coefficients evaluated at appropriate points. The solution of this forward problem can be used to remove the PDE constraint in the parameter identification problem. Thus, the PDE constrained minimization problem reduces to a simpler non-linear minimization problem.

The approach proposed in this study has been successfully applied to a river-reach in the Sacramento– San-Joaquin Delta, where the parameters of the linear Saint-Venant model as well as the steady state boundary conditions are estimated based on the measured flow variables at the boundaries.

REFERENCES

- [1] A. BENNETT, *Inverse methods in physical oceanography*. Cambridge university press, 1992.
- [2] L. LJUNG, *System identification – theory for the user*. Prentice Hall, 1999.
- [3] J. CUNGE, F. HOLLY, and A. VERWEY, *Practical aspects of computational river hydraulics*. Pitman, 1980.
- [4] X. Litrico and V. Fromion, “Frequency modeling of open channel flow,” *ASCE Journal of Journal of Hydraulic Engineering*, vol. 130, no. 8, pp. 806–815, 2004.
- [5] B. SANDERS, “High-resolution and non-oscillatory solution of the st. venant equations in non-rectangular and non-prismatic channels,” *Journal of Hydraulic Research*, vol. 39, no. 3, pp. 321–330, 2001.
- [6] I. Mareels and E. Weyer, “Systems engineering design for irrigation systems,” in *IFAC LSS Symposium*, 2004, plenary contribution.
- [7] G. HUG-GLANZMANN, M. VON SIEBENTHAL, T. GEYER, G. PAPAFOTIU, and M. MORARI, “Supervisory water level control for cascaded river power plants,” in *Hydropower Conference 05*, Norway, 2005.
- [8] Y. DING, Y. JIA, and S. WANG, “Identification of manning’s roughness coefficients in shallow water flows,” *J. Hydraul. Eng.*, vol. 130, no. 6, pp. 501–510, 2004.
- [9] M. NODET, “Variational assimilation of lagrangian data in oceanography,” *Inverse Problems*, vol. 22, pp. 245–263, 2006.
- [10] J.-L. Lions, *Optimal control of distributed systems*. Springer Verlag, 1970.
- [11] V. CHOW, *Open-channel Hydraulics*. McGraw-Hill Book Company.
- [12] X. LITRICO and V. FROMION, “Simplified modeling of irrigation canals for controller design,” *J. Irrig. Drain. Eng.*, vol. 130, no. 5, pp. 373–383, 2004.